analytical chemistry

Article

pubs.acs.org/ac

Electrostatic Spray Ionization from 384-Well Microtiter Plates for Mass Spectrometry Analysis-Based Enzyme Assay and Drug Metabolism Screening

Liang Qiao,[†,‡,#] Xiaoqin Zhong,[†,#] Emna Belghith,[†] Yan Deng,[†,§] Tzu-En Lin,[†] Elena Tobolkina,[†] Baohong Liu,[‡] and Hubert H. Girault*[,†]

[†]Laboratoire d'Electrochimie Physique et Analytique, Ecole Polytechnique Fédérale de Lausanne (EPFL), Rue de l'Industrie 17, CH-1951 Sion, Switzerland

[‡]Chemistry Department, Fudan University, 200433 Shanghai, China

[§]College of Chemistry and Molecular Engineering, Peking University, 100871 Beijing, China

Supporting Information

ABSTRACT: We have realized the direct ionization of samples from wells of microtiter plates under atmospheric conditions for mass spectrometry analysis without any liquid delivery system or any additional interface. The microtiter plate is a commercially available 384-well plate without any modification, working as a container and an emitter for electrostatic spray ionization of analytes. The approach provides high throughput for the large batches of reactions and both the qualitative and quantitative analysis of a single compound or mixture. The limits of detection in small drug molecules, peptides, and proteins are similar in comparison with standard direct infusion electrospray ionization. The analysis time per well is only seconds. These analytical merits benefit many microtiter plate-based studies, such as combinatorial chemistry and high throughput screening in enzyme assay or drug metabolism. Herein, we illustrate the application in enzyme assay using tyrosine oxidation catalyzed by tyrosinase in the presence or absence of inhibitors. The potential application in drug development is also demonstrated with cytochrome P450-catalyzed metabolic reactions of two drugs in microtiter plates followed with direct ESTASI-MS/MS-based characterization of the metabolism products.

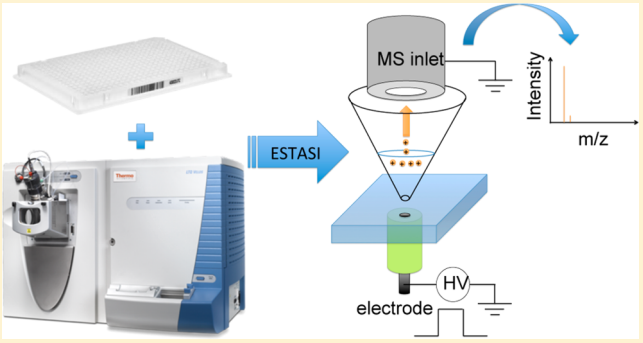

Microtiter plates are used as a standard tool in analytical chemistry, clinical assay, and life science study. Because of the large number of wells per plate, it is widely used for combinatorial chemistry and high throughput screening. Coupled with various chemical analysis techniques, such as ultraviolet−visible spectroscopy, fluorescence spectroscopy, liquid chromatography (LC), capillary electrophoresis (CE), and mass spectrometry (MS), it is extensively used for enzyme-linked immunosorbent assays (ELISA),[1] enzyme activity or inhibition assays,[2,3] and drug metabolism studies.[4,5] Compared to spectroscopy techniques, MS can offer direct qualification and quantification of a wide range of analytes, providing accurate and specific characterization to avoid false positive or negative results, and thereby is highly suitable for the studies of enzymatic assays, inhibitor screening assays, and drug metabolism assays.[6−10]

MS is normally coupled with microtiter plates with the help of liquid delivery robots. For instance, Advion has commercialized a TriVersa NanoMate system, which collects fractions during LC-MS in a 96- or 384-well plate, that are later analyzed by electrospray ionization (ESI) MS via an ESI chip. This system has been used in lipidomic studies, screening of drug metabolism, protein−ligand interaction study, biotherapeutics, etc.[11−14] In a more common way, autosamplers from various suppliers are used in coupling microtiter plates with MS. However, the use of autosamplers limits the throughput of analyses, especially in comparison with spectroscopy-based microtiter plate assays. There have been a lot of efforts spent to modify autosamplers to overcome the disadvantage. A multiprobe autosampler was developed by Kassel et al. to couple with flow injection MS, where the analysis of a whole 96-well plate could be finished in 12 min instead of 48 min by a single-probe autosampler.[15] Later on, it was further optimized by Morand et al. to finish the analysis of a 96-well plate in 5 min.[16] Another option is avoiding using autosamplers all together, but with a ESI interface for direct infusion and ionization of samples from a microtiter plate for MS analysis.[17,18] Recently, Trimpin et al. have presented direct

Received: February 13, 2017
Accepted: April 28, 2017
Published: April 28, 2017

DOI: 10.1021/acs.analchem.7b00536
Anal. Chem. 2017, 89, 5983−5990

ionization from a 96-well plate by a solvent assisted ionization inlet (SAII), where disposable micropipette tips were modified on each well of the 96-well plate to form an ionization device with the original wells as containers and the pipet tips as emitters.[19]

Herein, we have realized direct ionization of liquid samples from an unmodified microtiter plate, where the plate itself works as both containers and emitters for ionization. To the best of the authors' knowledge, it is the first method of direct ionization from a microtiter plate without any liquid delivery interface and any modification to the plate. The ionization is achieved using the recently developed electrostatic spray ionization (ESTASI).[20−22] The microtiter plate is simply placed between the ion transfer capillary of a mass spectrometer and the electrode connected to a pulsed high voltage (HV) power source. When the pulsed HV is applied, ESTASI occurs to generate alternative spray of cations and anions for MS analysis.[20]

The performance of the ionization for qualification and quantification was evaluated. Different types of samples, including small drug molecules, amino acids, peptides, and proteins could be detected with limits of detection (LOD) similar to those of standard direct infusion ESI. Quantitative analysis was also realized by adding a proper internal standard into the tested sample. Because the microtiter plate is disposable and no liquid delivery is needed, washing steps can be avoided to shorten analysis time and eliminate cross-contamination between samples. The analysis time per well is only few seconds to generate a mass spectrum. With these advantages, the technique is highly suitable for fast analysis of a single compound or mixture. In addition, it holds potential applications in high throughput assays, such as enzyme inhibition screening and drug metabolism studies. To illustrate these, tyrosinase-catalyzed oxidation of tyrosine with or without inhibitors and *in vitro* drug metabolism by cytochrome P450 in microtiter plates were directly read by ESTASI-MS.

EXPERIMENTAL SECTION

Chemicals and Materials. Ciprofloxacin (CIP), enrofloxacin (ENR), lomefloxacin (LOM), and fleroxacin (FLE) of analytical reagent grade were purchased from TCI Deutschland GmbH (Eschborn, Germany). Angiotensin I (Ang I, 98%) was obtained from Bachem (Bubendorf, Switzerland). Cytochrome c (Cyt c, horse heart, 95%), magnesium chloride hexahydrate (98%), sodium phosphate dibasic dodecahydrate (99%), sodium phosphate monobasic (99%), and sodium chloride (99.5%) were obtained from Fluka (St. Gallen, Switzerland). Methanol (99.9%, HPLC grade) was purchased from Applichem GmbH (Darmstadt, Germany). Acetic acid (HAc, 99%) was obtained from Merck (Zug, Switzerland). Ammonium bicarbonate (NH_4HCO_3, 99%,), calcium chloride (93%), tyrosinase (from mushroom, lyophilized powder, ≥1000 unit/mg solid), L-tyrosine (99%), reduced nicotinamide adenine dinucleotide phosphate (NADPH), nifedipine (≥98%, powder), testosterone (≥98%, powder), and cytochrome P450 CYP3A4 isozyme microsomes expressed in baculovirus-infected cells were purchased from Sigma-Aldrich (St. Gallen, Switzerland). Potassium chloride (99%) was obtained from Roth AG (Arlesheim, Switzerland). Cupferron (for analysis) was purchased from Fisher Scientific (Waltham, MA, USA). All these reagents and materials were used as received without further purification. Deionized water (18.2 MΩ cm) was obtained from an ultrapure water system (Milli-Q 185 Plus, Millipore) and used for all experiments. A MicroAmp optical 384-well reaction plate with a barcode was purchased from life technologies (Carlsbad, CA, USA).

Tyrosine Oxidation and Drug Metabolism. Wells of a 384-well microtiter plate were filled with 8 μL of phosphate buffered saline (PBS, 2 mM, pH 7.4), 1 μL of tyrosinase (0.2 mg/mL in 2 mM PBS), and 1 μL of tyrosine (0.5 mg/mL in 2 mM PBS). The detection by ESTASI-MS was directly performed from the wells at different time intervals to monitor the oxidation results. When enzyme inhibition was studied, 1 μL of ascorbic acid (AA, 1 or 0.1 mg/mL in 2 mM PBS), or 1 μL of Cupferron (20 mM in 2 mM PBS) was added, followed by the addition of 7 μL of PBS (2 mM), 1 μL of tyrosinase (0.2 mg/mL in 2 mM PBS), and 1 μL of tyrosine (0.5 mg/mL in 2 mM PBS).

For drug metabolism, 80 μg/mL of nifedipine or 40 μg/mL of testosterone was prepared in 10 mM NH_4HCO_3 (pH 7.4), respectively. NADPH (1 μL of 50 mg/mL in 10 mM NH_4HCO_3), 1 μL of CYP3A4 (1 μM in 100 mM KH_2PO_4, pH 7.4), and 8 μL of the drug solution were added in multiple wells of a 38-well plate. After being incubated for different periods at room temperature, 9 μL of the reaction solution was discarded and 9 μL of 50% MeOH/49% H_2O/1% acetic acid was added for ESTASI-MS analysis.

ESTASI-MS. ESTASI-MS was performed as described in previous publications[20,23] and illustrated by Figure 1. A 384-well plate was placed on a PET substrate (120 μm thickness), and all together between an electrode and the ion transfer capillary of a linear ion trap mass spectrometer (LTQ Velos, Thermo scientific). The ion transfer capillary was a self-designed "L-shaped" ion transfer capillary instead of the original linear one of the MS instrument, which could maintain a Convectron Gauge value of 1 Torr for good ion transfer into the mass spectrometer. The modification was carried out in order to place the microtiter plate horizontally for MS analysis. The plate was moved in *x*, *y*, and *z* directions by travel translation stages to bring different wells under the ion transfer capillary. A pulsed high voltage (HV, from 0 V to 8 kV, frequency 20 Hz) was generated by amplifying voltage square wave pulses (0 to 8 V) with a high voltage amplifier (10HVA24-P1, HVP High Voltage Products GmbH, Martinsried/Planegg, Germany), and applied on the electrode to induce ESTASI against the ion transfer capillary that was set at 275 °C and always grounded. The ESI voltage of the internal power of the MS instrument was always set as 0, and all the source gas flow rates were set at 0. An enhanced ion trap scanning rate of 10,000 *m*/*z* per second was used. The other parameters of the MS instrument were optimized for the

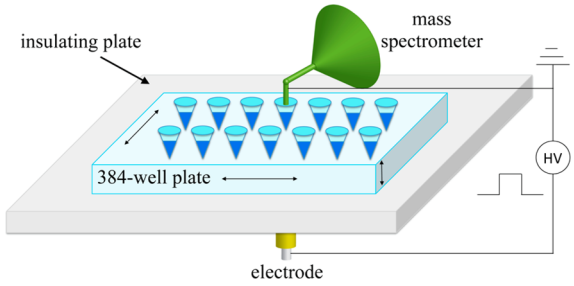

Figure 1. Schematic representation of the setup used for ESTASI-MS from a 384-well plate. HV: high voltage, which is a square wave pulsed HV here.

DOI: 10.1021/acs.analchem.7b00536
Anal. Chem. 2017, 89, 5983−5990

selected analytes and not described here. All MS analyses were performed under positive scanning mode. For the collision-induced dissociation (CID), full scan mode was performed with a normalized collision energy of 30 and isolation width of 1 *m/z*.

Direct Infusion ESI. For sensitivity comparison, samples were also analyzed via a direct infusion mode ESI with a syringe at the flow rate of 3 μL/min. The ESI was performed with the commercially equipped ESI source of LTQ velos with a spray emitter of 500 μm in diameter and assisted by a sheath gas flow of 10 arbitrary units and auxiliary gas flow of 5 arbitrary units. The ESI voltage was 3.7 kV. The temperatures of the heater and the MS inlet capillary were set at 42 and 275 °C, respectively. All other parameters of the MS instrument were the same as those for ESTASI analysis.

RESULTS AND DISCUSSION

384-Well Plate ESTASI-MS. According to the previous studies, ESTASI occurs during electrostatic charging/discharging of the capacitors formed by (i) an electrode−insulator−electrolyte solution and (ii) an electrolyte solution−gas−ion transfer capillary.[20] Charge separation happens inside the electrolyte solution during charging of the capacitors, e.g. anions to the part close to the electrode and cations to the part close to the ion transfer capillary when a positive HV is applied on the electrode. When the charge density on the part close to the ion transfer capillary is large enough, electrospray of cations occurs. Afterward, spray of anions can be induced by simply grounding the electrode to make the electrolyte solution neutral. According to this ionization principle, it is crucial to reach a large charge density to start ESTASI that can be realized either by increasing the charge amount accumulated on the part of the electrolyte solution close to the ion transfer capillary or by reducing the surface area of the region. The charge amount can be increased by increasing the HV, increasing the surface area of the electrode, decreasing the thickness of the insulator, and decreasing the distance from the electrolyte solution to the ion transfer capillary.[20]

ESTASI has been realized with various setups, e.g. microchip ESTASI, gel strip ESTASI, and ESTASI MS imaging from an insulating plate.[21,22,24] When the solution is inside the wells of a microtiter plate, its surface area exposed to the ion transfer capillary is determined by the shape of the well. A typical 96-well plate has normally quasi-cylindrical wells (about 8 mm Ø) with the volume up to 1 mL each, resulting in a large area of sample solution inside exposed to the ion transfer capillary during ESTASI. Indeed, it is very difficult to perform direct ESTASI of samples from a normal 96-well plate. Herein, we chose a commercially available 384-well plate with cone-shaped wells that had the volume of 40 μL each with the diameter of 3 mm at the base of the cone. When 10 μL of sample solution was filled in a well for ESTASI-MS analysis, the liquid exposed to the ion transfer capillary was discal-shaped with a diameter less than 2 mm. The ion transfer capillary probed into the well and kept the distance of 1−2 mm from the sample to avoid sucking the sample solution into the capillary by vacuum (Supporting Information Video 1). As soon as the pulsed HV was applied on the electrode, ESTASI happened to produce ions for MS analysis. Without the pulsed HV, no signal was observed by the mass spectrometer. During ESTASI, the sample was consumed, resulting in enlarging the distance between the ion transfer capillary and the sample solution. This would decrease the charge amount on the liquid surface, and finally stop ESTASI. Therefore, the 384-well plate should be lifted up carefully during ESTASI until all the sample solution in the well was exhausted. The consumption of 10 μL of sample solution normally needed 30 s. The analysis of many wells was performed with the help of an *x, y, z* translation system.

The 384-well plate ESTASI-MS was tested with different samples, including small organic molecules, peptides, and proteins. A group of synthetic antibiotics derived from quinolone nalidixic acid, including ciprofloxacin (CIP), enrofloxacin (ENR), lomefloxacin (LOM), and fleroxacin (FLE), were selected as examples of small organic drug molecules. These antibiotics were introduced for the therapeutic treatment of respiratory and urinary infections since the mid-1990s.[25] The extensive use of the antibiotics has led to their accumulation in food, which has potential health hazards for humans.[26] Therefore, it is highly important to develop analytical techniques for the detection of trace amounts of the antibiotics. As shown in Figure 2(a), an intense peak of

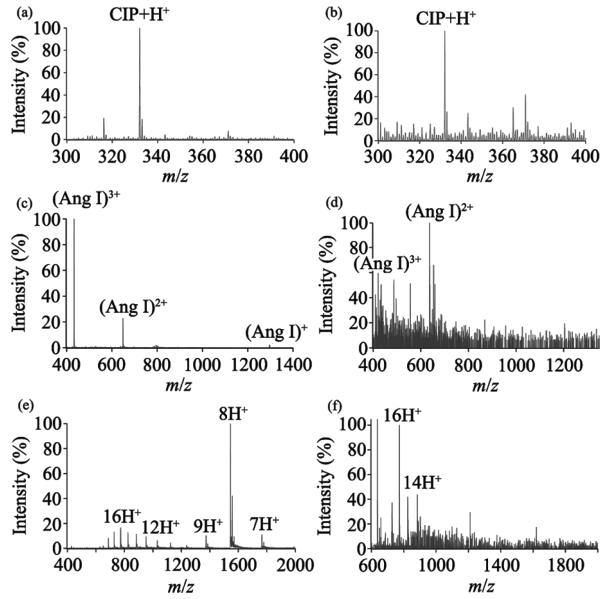

Figure 2. Mass spectra obtained by the 384-well plate ESTASI-MS of (a) 1.5 μM CIP, (b) 15 nM CIP, (c) 15 μM Ang I, (d) 15 nM Ang I, (e) 10 μM Cyt c, and (f) 100 nM Cyt c. Solution: 50% MeOH/49% H_2O/1% acetic acid. CIP + H^+: singly protonated CIP; $(Ang\ I)^{x+}$: Ang I ion with *x* proton(s); XH^+: Cyt c ion with *x* proton(s).

the single protonated CIP was obtained from 1.5 μM CIP in 50% MeOH/49% H_2O/1% acetic acid by the 384-well plate ESTASI-MS. When the concentration of CIP was lowered to 15 nM, the peak was still clearly observed with the signal-to-noise (S/N) ratio >10 (Figure 2(b) and Table 1). Detection of other antibiotics was also performed. When 1.4 μM LOM, FLE, and ENR were used, peaks for the single protonated antibiotics were easily observed. When the concentration was lowered to 140 nM, the peaks could still be observed but with the S/N of only 4, 2, and 3 for LOM, FLE, and ENR, respectively (Table 1 and Supporting Information (SI) Figures SI-1, SI-2, and SI-3). The results were compared with standard direct infusion ESI-MS analysis of the same samples by the same linear ion trap mass spectrometer (Thermo, LTQ Velos). Similar LOD was demonstrated under the optimized instrumental conditions (Table 1).

DOI: 10.1021/acs.analchem.7b00536
Anal. Chem. 2017, 89, 5983−5990

Table 1. Comparison of the Detection of Antibiotics Ang I and Cyt c by 384-Well Plate ESTASI-MS and Standard Direct Infusion ESI-MS

Compound	Method	m/z	LOD	S/N
CIP	ESTASI-MS	332	15 nM	>10
CIP	ESI-MS	332	15 nM	3
LOM	ESTASI-MS	352	140 nM	4
LOM	ESI-MS	352	140 nM	4
FLE	ESTASI-MS	370	140 nM	2
FLE	ESI-MS	370	140 nM	3
ENR	ESTASI-MS	360	140 nM	3
ENR	ESI-MS	360	140 nM	5
Ang I	ESTASI-MS	649[a]	15 nM	5
Ang I	ESI-MS	433[b]	50 nM	10
Cyt c	ESTASI-MS	773[c]	100 nM	10
Cyt c	ESI-MS	773[c]	70 nM	10

[a]Doubly protonated angiotensin I. [b]Triply protonated angiotensin I. [c]Cyt c with 16 protons.

Peptide (angiotensin I (Ang I), 1295 Da) was also tested by the 384-well plate ESTASI-MS. As illustrated in Figure 2(c), a mass spectrum similar to that from the standard direct infusion ESI-MS was obtained from 15 μM Ang I in 50% MeOH/49% H_2O/1% acetic acid. The LOD of Ang I by the 384-well plate ESTASI-MS was found to be about 15 nM, where a peak at m/z 649 for the doubly protonated Ang I was observed with the S/N of 5 (Figure 2(d)). In contrast, standard infusion mode ESI-MS needs at least 50 nM of Ang I to generate a clear peak (S/N = 10) of the peptide at m/z 433 for the triply protonated ion (Table 1).

The analysis of proteins by the 384-well plate ESTASI-MS was demonstrated using cytochrome c from horse heart (Cyt c, 12 kDa). When the concentration of Cyt c was high (10 μM in 50% MeOH/49% H_2O/1% acetic acid), the obtained mass spectrum showed the strongest peak at m/z 1546 for the protein ions with 8 protons (Figure 2(e)). The LOD was found at 100 nM of Cyt c, with the strongest peak (S/N = 10) at m/z 773 for the protein ions with 16 protons. Direct infusion mode ESI-MS provides the LOD of Cyt c (70 nM), slightly better than the 384-well plate ESTASI-MS, with also the strongest peak (S/N = 10) at m/z 773 (Table 1).

As shown in Table 1, different samples show different LODs with the 384-well plate ESTASI-MS. The technique shows the lowest LODs for CIP and Ang I, which are relatively small in size and have basic amino groups (pK_a = 8.68 for CIP and 8 for Ang I) for protonation. ENR and FLE have the pK_a of 6.68 and 6.06, respectively, making the protonation rather difficult and hence leading to high LODs. Cyt c is big in size and can only be observed by ion trap mass spectrometer when it is highly charged. When a cone-shaped well of a 384-well plate works as a spray emitter for ESTASI, the solution exposed to ion transfer capillary is discal-shaped with a diameter of 1−2 mm. The increased emitter size will lead to low surface charge density. During the analysis of proteins, the charge number tended to low numbers to generate ions with large mass-to-charge ratio values, which were difficult to be detected by the ion trap mass spectrometer. In general, the method is as sensitive as standard direct infusion ESI-MS in the analysis of small organic molecules and peptides, but less sensitive against proteins.

However, different from the standard ESI-MS, the 384-well plate ESTASI-MS can provide higher throughput and lower sample consumption in analysis. During 384-well plate ESTASI-MS, the sample volume in each well is normally from 2 to 10 μL. The ionization device is simply a disposable microtiter plate, where washing procedures are not required from one analysis to the next. The analysis time per well is only a few seconds to generate a mass spectrum. In contrast, direct infusion ESI-MS requires either a LC autoinjector or continuous syringe injection. In both cases of direct infusion ESI-MS, washing of the liquid delivery part is required after each analysis, which is time-consuming, especially when the analytes are strongly adsorbed by the tubing system.

Enzyme Inhibition Assay by 384-Well Plate ESTASI-MS. One of the potential applications of the 384-well plate ESTASI-MS is the enzyme assay study. MS has drawn increasing interest in enzyme activity assays and enzyme inhibition assays during the last years.[6] Compared to spectroscopy-based methods, the MS strategy does not need expensive labeling reagents, and provides highly accurate identification to avoid false positive results. Both laser desorption/ionization (LDI) and electrospray ionization (ESI)-based MS techniques are used for enzyme assay study.[8,27] The former holds the advantage of high throughput, but difficulty in quantification. The later provides better quantification, but is limited by throughput. ESTASI was demonstrated as a concentration-dependent ionization technique, similar to ESI, suitable for quantification.[22] Therefore, the 384-well plate ESTASI-MS can hold both the advantages of quantitative analysis, like ESI-MS, and high throughput, like LDI-MS. By avoiding the washing procedure, the time to analyze a sample is only seconds.

The quantitative capability of 384-well plate ESTASI-MS was demonstrated by detecting tyrosine of different concentrations. The classical method of internal standard calibration was used for tyrosine quantification, where serine was chosen as the internal standard. The high correlation coefficient value (R^2 = 0.992) obtained from the fitted curve in Figure SI-4 of the SI indicates the good linear response of the relative ion intensities to the tyrosine concentrations within the range 2−50 mg/L, demonstrating the concentration-dependent ionization performance of the 384-well plate ESTASI-MS.

To demonstrate the application in an enzyme assay, we performed the oxidation of tyrosine in the presence of tyrosinase without and with inhibitors, followed by ESTASI-MS analysis. Oxidation of tyrosine catalyzed by tyrosinase, peroxidases, or haem-containing proteins can form DOPA, 5,6-dihydroxyindole (5,6-DHI), and finally melanin,[28] as show in Scheme 1. It is also involved in browning reactions in damaged fruits.[29] A number of wells were prepared containing tyrosine (0.05 mg/mL) and tyrosinase (0.02 mg/mL) in 2 mM PBS (pH 7.4), and incubated at room temperature for various periods before ESTASI-MS analysis. After 3 min of reaction, a clear peak for single protonated 5,6-DHI at m/z 150 was

Scheme 1. Oxidation of Tyrosine Catalyzed by Tyrosinase

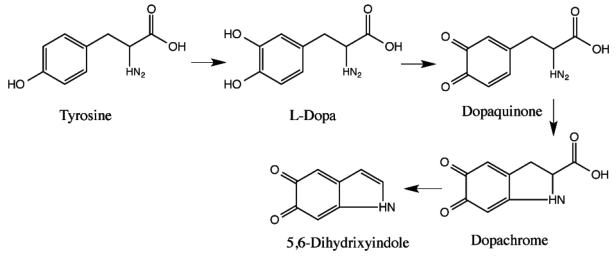

DOI: 10.1021/acs.analchem.7b00536
Anal. Chem. 2017, 89, 5983−5990

observed in Figure 3(a), together with a peak for singly protonated tyrosine at m/z 182. The other oxidation products

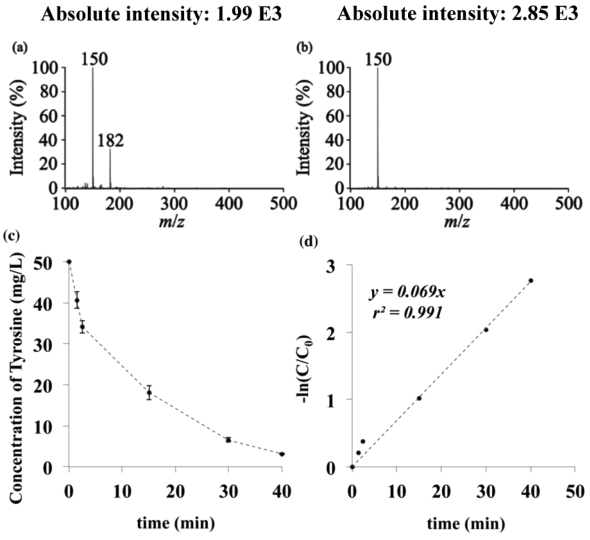

Figure 3. Mass spectra of the products of tyrosine (0.05 mg/mL) oxidation catalyzed by tyrosinase (0.02 mg/mL) after (a) 3 min and (b) 20 min of reaction. (c) Concentration variation of tyrosine during the enzyme-catalytic oxidization within 40 min. (d) Reaction kinetics of tyrosine oxidation. The reaction was performed in the wells of a 384-well plate followed with direct ESTASI-MS analysis in a buffer condition of 2 mM PBS at pH 7.4. Error bars show standard deviation (n = 3).

were hardly observed, indicating that they were quickly consumed after formation to produce 5,6-DHI or hardly ionized for MS analysis. During ESTASI-MS analysis, the buffer was 2 mM PBS at pH 7.4. Prolonging the reaction time, the tyrosine concentration continued to decrease slowly. After 20 min of reaction, only a very weak peak of tyrosine was obtained in Figure 3(b), indicating that most of the reactant was consumed. The reaction kinetics was analyzed based on the classic Michaelis–Menten kinetic process[30] and followed a pseudo-first-order reaction with the reaction rate constant of 0.069 min^{-1}, indicating that the Michaelis constant K_M is much larger than the substrate (tyrosine) concentration (0.05 mg/mL) in this case (Figure 3(c) and (d)).

The inhibition of tyrosinase-catalyzed tyrosine oxidation is an important topic in food and cosmetic chemistry to avoid hyperpigmentation in human skin and enzymatic browning in fruits or fungi.

Recently developed inhibitors have been summarized in several reviews.[29,31,32] In this work, we used two inhibitors, ascorbic acid and Cupferron, to illustrate the feasibility of applying the 384-well plate ESTASI-MS in enzyme inhibition assays. Ascorbic acid is an antioxidant, working as an inhibitor of many enzymatic oxidative reactions. The enzyme inhibition assay was performed by preparing a number of wells containing ascorbic acid at different concentrations (0.1 and 0.01 mg/mL) with tyrosine (0.05 mg/mL) and tyrosinase (0.02 mg/mL) in 2 mM PBS, followed by ESTASI-MS analysis after different times of incubation. As shown in Figure 4(a), tyrosine oxidation was efficiently inhibited by 0.01 mg/mL ascorbic acid within 20 min of incubation, but the tyrosine concentration started to decrease sharply when prolonging the incubation time and was almost completely consumed after 40 min. It suggests that ascorbic acid works as a competitive inhibitor, continuously consumed during the enzymatic reaction. In contrast, with a higher concentration of ascorbic acid (0.1 mg/mL), the inhibition can last effectively for at least 40 min (in Figure 4(b)). Therefore, a successful and continuous inhibition requires the proper amount of ascorbic acid or the addition of ascorbic acid round-the-clock.

Cupferron is a metal-chelating agent that can coordinate the copper ion of mushroom tyrosinase to inhibit completely its activity.[33] Replacing ascorbic acid by Cupferron, the inhibition was studied by 384-well plate ESTASI-MS. As a competitive inhibitor, the concentration of Cupferron should be sufficiently higher than that of tyrosine for the efficient inhibition of tyrosinase (0.15 μM). Theoretically, at least 1 mM of Cupferron is required for complete inhibition of tyrosinase in the presence of 0.3 mM tyrosine through calculation of the half maximal inhibitory concentration (IC_{50}), in the SI. Herein, 2 mM Cupferron was applied to ensure maximum inhibition of tyrosinase. As shown in Figure 4(c), no oxidation product was observed after 10 min of reaction. With longer incubation time, the oxidation was still not observed by ESTASI-MS, consistent with the proposed inhibition mechanism that Cupferron completely deactivates tyrosinase. The strong peak in Figure 4(c) at m/z 157 was from Cupferron, which was also observed by standard direct infusion ESI-MS of pure Cupferron in 50% MeOH/49% H_2O/1% acetic acid (Figure SI-5).

Drug Metabolites Screening by the 384-Well Plate ESTASI-MS. Another important application of the 384-well plate is drug candidate screening. In-vitro studies of the drug

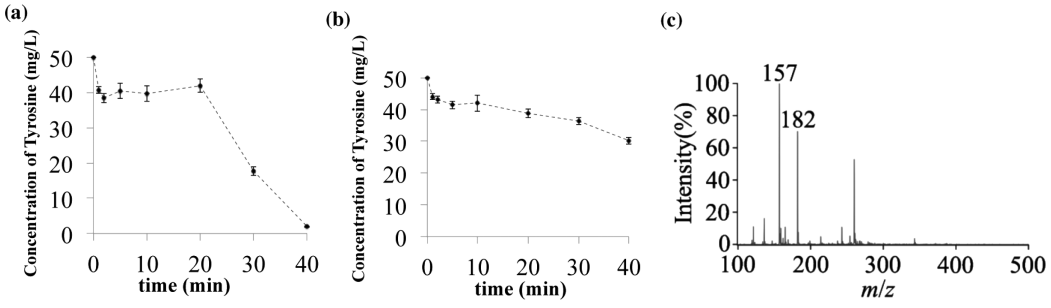

Figure 4. Tyrosinase inhibition assay with different amounts of ascorbic acid as the inhibitor: (a) 0.01 mg/mL of ascorbic acid; (b) 0.1 mg/mL of ascorbic acid. (c) Mass spectrum obtained after 10 min of reaction inhibited by 2 mM of Cupferron. The reactions were performed in 10 μL solutions containing 0.05 mg/mL of tyrosine, 0.02 mg/mL of tyrosinase, and different amounts of inhibitors in a buffer of 2 mM PBS at pH 7.4 in the wells of a 384-well plate followed by direct ESTASI-MS analysis.

DOI: 10.1021/acs.analchem.7b00536
Anal. Chem. 2017, 89, 5983−5990

candidate metabolism could predict its potential toxicity, which is crucial in early stage drug discovery.[34] The rapid developments of combinatorial chemistry and advances in bioinformatics, genomics, and proteomics have driven the potential targets for new drug development increase dramatically in the past decade.[35] Therefore, low cost, rapid and high throughput drug candidate screening methods are urgently needed. 384-well plate screening combined with ESTASI-MS or ESTASI-MS/MS can be applied in drug candidate screening by characterizing the metabolites of drug candidates in a high throughput manner.

To demonstrate this application, cytochrome P450, one major family of human liver microsome enzymes widely used for *in vitro* metabolism and toxicity studies,[36] was chosen to induce drug metabolism in the wells of microtiter plates, while nifedipine and testosterone were used as substrates. Nifedipine is a prototype of the dihydropyridine class of calcium channel blockers that is widely used in the treatment of hypertension, prinzmtal's angina pectoris, and other vascular disorders,[37] while testosterone is a male sex hormone that is important for sexual and reproductive development and plays a vital role in carbohydrate, fat, and protein metabolism.[38]

The CYP3A4-catalyzed metabolisms of both nifedipine and testosterone were simultaneously studied by 384-well plate ESTASI-MS during a single run analysis. In both cases, NADPH was added as an electron donor. Multiple wells in a 384-well plate were filled with 10 μL of solutions, each containing 64 μg/mL of nifedipine or 32 μg/mL of testosterone, 1 mg/mL of NADPH, and 0.1 μM CYP3A4 in 10 mM NH_4HCO_3 (pH 7.4). The solutions were incubated for a certain time under room temperature and then directly analyzed by ESTASI-MS at different time intervals. The tolerance to a salty solution of the 384-well plate ESTASI-MS was estimated be around 30 mM NaCl for the analysis of 50 nM Ang I, as shown in Figure SI-6. Considering that the high concentration of salts (around 30 mM) in the reaction solution could hinder the efficient detection of the drugs and their metabolic products, 9 μL of the reaction mixture was discarded and replaced by 9 μL of the ionization buffer (50% MeOH/49% H_2O/1% acetic acid) for ESTASI-MS analysis.

The primary product of nifedipine metabolism catalyzed by CYP3A4 is dehydronifedipine with the m/z at 345, as shown in Scheme 2(a) and Figure 5(d), which is consistent with the literature report.[37] After 30 min of incubation, the majority of nifedipine was oxidized, and the conversion ratio reached around 70%, as shown in Figure 5(a). When prolonging the reaction time to 90 min, little nifedipine was further oxidized. A linear regression was obtained in Figure 5(b) and the nifedipine oxidation could be considered as the pseudo-first-order reaction. Within 30 min, the reaction rate constant was determined as 0.037 min^{-1}, in Figure 5(b).

Structural elucidation of drug candidate metabolic products could facilitate the prediction of its toxicity based on the regression model of quantitative structure−toxicity relationship (QSTR), which relates the structure variables to the potency of toxicity variables.[39] For this purpose, tandem MS with collision-induced dissociation (CID) was further applied to characterize the structure of the oxidized nifedipine. With normalized collision energy of 30, the precursor ion of m/z 345 generated a predominant fragment ion with m/z 284, corresponding to the loss of CH_3COOH from the metabolic product, in Figure 5(e). Both the precursor ion and the fragments indicated the generation of dehydronifedipine.

Metabolic oxidation of testosterone was also monitored in the same 384-well plate together with nifedipine during a single run of analysis. From Scheme 2(b) and Figure 6(d), the testosterone metabolism generated hydroxytestosterone and 6β-hydroxytestosterone is the primary structure, according to the literature report.[38] Figure 6(a) and (b) presented the oxidation process and only 40% of conversion ratio was obtained until 90 min of incubation. A reaction rate constant was obtained as 0.0072 min^{-1} for the metabolism of testosterone (Figure 6(b)). The corresponding mass spectra of the testosterone and its oxidation product are shown in Figure 6(c) and (d). The metabolic product ion with m/z 305 was selected for the CID process and generated the primary fragments by the detachment of two −OH groups, confirming the formation of hydroxytestosterone (Figure 6(e)).

These results show that the 384-well plate ESTASI-MS/MS provides the possibility to directly characterize metabolic products in a high speed and throughput way without any solution purification or delivery interface. The 384-well plate ESTASI-MS and ESTASI MS/MS will be of great value in rapid and accurate *in vitro* drug metabolism study and toxicity prediction.

Scheme 2. Oxidative Metabolism of (a) Nifedipine and (b) Testosterone Catalyzed by Cytochrome P450 CYP3A4

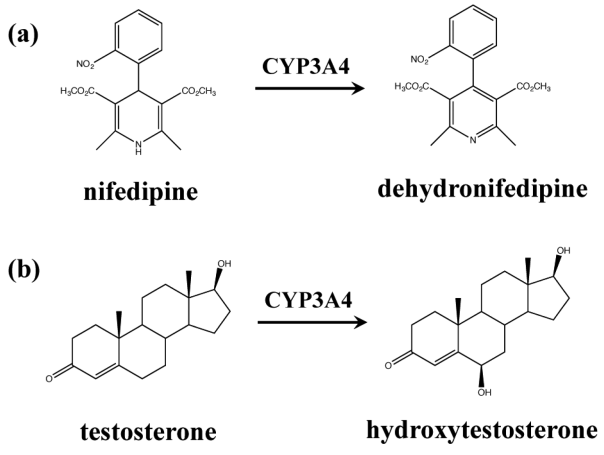

CONCLUSION

In conclusion, we have realized direct ionization of liquid samples inside a microtiter plate by electrostatic spray ionization. Analytical characteristics, including sensitivity and quantification capability, were evaluated. The method can be universally applied for a wide range of samples, from organic molecules with molecular weights of ~150 Da to proteins of >10 kDa. The ionization device is demonstrated as efficient as standard ESI in view of sensitivity to trace amount of analytes, while it also holds advantages in analysis throughput. Two applications were further explored: enzyme assay and drug metabolism screening. We would expect the current ionization method to be a powerful tool in high throughput MS-based enzyme activity assays, enzyme inhibition assays, immunoassays, and drug candidate screenings.

DOI: 10.1021/acs.analchem.7b00536
Anal. Chem. 2017, 89, 5983−5990

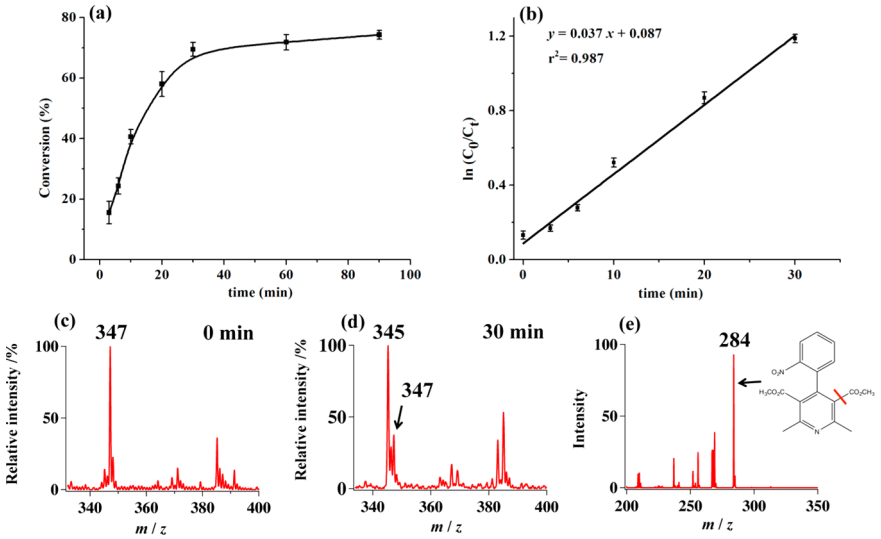

Figure 5. Fitted curves and mass spectra for CYP3A4-catalyzed metabolism of nifedipine. (a) Conversion ratio of nifedipine as a function of time. (b) Reaction kinetics of nifedipine metabolism. (c and d) Mass spectra of nifedipine and its metabolites before reaction and after 30 min of reaction, respectively. (e) CID spectrum of the precursor ion at m/z 345 with normalized collision energy of 30 and isolation width of 1 m/z. The reactions were performed with 64 μg/mL of nifedipine, 1 mg/mL of NADPH, and 0.1 μM of CYP3A4 in 10 μL of 10 mM NH_4HCO_3 (pH 7.4) in a 384-well plate. Nine μL of the reaction solution was discarded and replaced with 9 μL of the ionization buffer (50% MeOH/49% H_2O/1% acetic acid) prior to ESTASI-MS analysis.

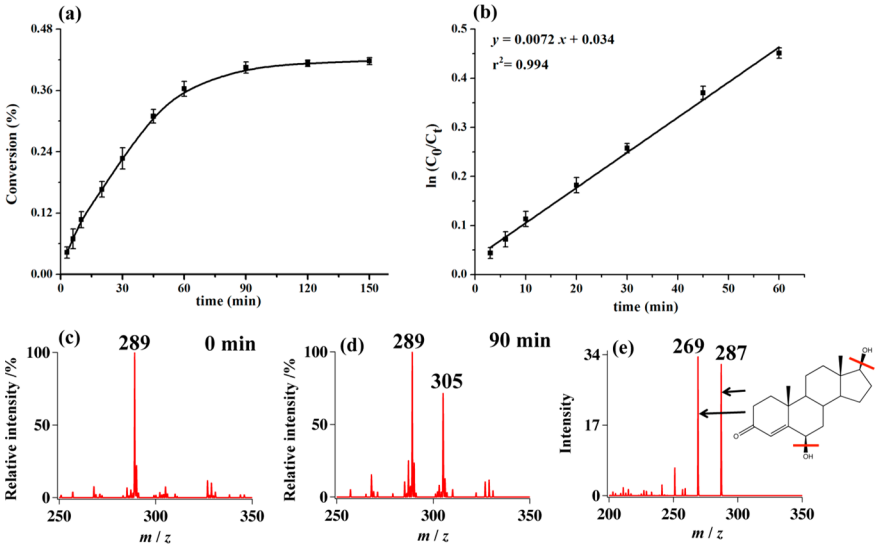

Figure 6. Fitted curves and mass spectra for the CYP3A4-catalyzed metabolism of testosterone. (a) Conversion ratio of testosterone as a function of time. (b) Reaction kinetics of testosterone metabolism. (c and d) Mass spectra of testosterone and its metabolites before reaction and after 90 min reaction, respectively. (e) CID spectrum of the precursor ion at m/z 305 with normalized collision energy of 30 and isolation width of 1 m/z. The reactions were performed with 32 μg/mL of nifedipine, 1 mg/mL of NADPH, and 0.1 μM of CYP3A4 in 10 μL of 10 mM NH_4HCO_3 (pH 7.4) in a 384-well plate. Nine μL of the reaction solution was discarded, replaced with 9 μL of the ionization buffer (50% MeOH/49% H_2O/1% acetic acid) prior to ESTASI-MS analysis.

■ ASSOCIATED CONTENT

Supporting Information

The Supporting Information is available free of charge on the ACS Publications website at DOI: 10.1021/acs.analchem.7b00536.

Mass spectra of LOM, FLE, and ENR by 384-well plate ESTASI-MS; fitted curve and mass spectra for tyrosine quantification; and mass spectrum of Cupferron by direct infusion ESI-MS; tolerance to salt of 384-well plate ESTASI-MS (PDF)

Video of sample suction by the ion transfer capillary (AVI)

■ AUTHOR INFORMATION

Corresponding Author

*E-mail: hubert.girault@epfl.ch.

ORCID

Liang Qiao: 0000-0002-6233-8459

Xiaoqin Zhong: 0000-0001-6964-7185

Author Contributions

#L.Q. and X.Z. contributed equally to the work.

DOI: 10.1021/acs.analchem.7b00536
Anal. Chem. 2017, 89, 5983−5990

Notes

The authors declare no competing financial interest.

■ ACKNOWLEDGMENTS

Xiaoqin Zhong and Yan Deng thank the Chinese Scholarship Council (CSC) for financial support. Tzu-En Lin thanks the Government Funds of Ministry of Education, Taiwan.

■ REFERENCES

(1) Cho, Y. A.; Kim, Y. J.; Hammock, B. D.; Lee, Y. T.; Lee, H. S. *J. Agric. Food Chem.* **2003**, *51*, 7854−7860.
(2) Palamanda, J. R.; Favreau, L.; Lin, C. C.; Nomeir, A. A. *Drug Discovery Today* **1998**, *3*, 466−470.
(3) Brik, A.; Wu, C. Y.; Wong, C. H. *Org. Biomol. Chem.* **2006**, *4*, 1446−1457.
(4) Kariv, I.; Fereshteh, M. P.; Oldenburg, K. R. *J. Biomol. Screening* **2001**, *6*, 91−99.
(5) Barros, A.; Ly, V.; Chando, T. J.; Ruan, Q. A.; Donenfeld, S. L.; Holub, D. P.; Christopher, L. J. *J. Pharm. Biomed. Anal.* **2011**, *54*, 979−986.
(6) Greis, K. D. *Mass Spectrom. Rev.* **2007**, *26*, 324−339.
(7) Liesener, A.; Karst, U. *Anal. Bioanal. Chem.* **2005**, *382*, 1451−1464.
(8) Hsieh, F.; Keshishian, H.; Muir, C. *J. Biomol. Screening* **1998**, *3*, 189−198.
(9) Xu, R. N. X.; Fan, L. M.; Rieser, M. J.; El-Shourbagy, T. A. *J. Pharm. Biomed. Anal.* **2007**, *44*, 342−355.
(10) Lahoz, A.; Donato, M. T.; Picazo, L.; Gomez-Lechon, M. J.; Castell, J. V. *Toxicol. In Vitro* **2007**, *21*, 1247−1252.
(11) Benkestock, K.; Van Pelt, C. K.; Akerud, T.; Sterling, A.; Edlund, P. O.; Roeraade, J. *J. Biomol. Screening* **2003**, *8*, 247−256.
(12) Staack, R. F.; Varesio, E.; Hopfgartner, G. *Rapid Commun. Mass Spectrom.* **2005**, *19*, 618−626.
(13) Schwudke, D.; Hannich, J. T.; Surendranath, V.; Grimard, V.; Moehring, T.; Burton, L.; Kurzchalia, T.; Shevchenko, A. *Anal. Chem.* **2007**, *79*, 4083−4093.
(14) Prien, J. M.; Prater, B. D.; Qin, Q.; Cockrill, S. L. *Anal. Chem.* **2010**, *82*, 1498−1508.
(15) Wang, T.; Zeng, L.; Strader, T.; Burton, L.; Kassel, D. B. *Rapid Commun. Mass Spectrom.* **1998**, *12*, 1123−1129.
(16) Morand, K. L.; Burt, T. M.; Regg, B. T.; Chester, T. L. *Anal. Chem.* **2001**, *73*, 247−252.
(17) Felten, C.; Foret, F.; Minarik, M.; Goetzinger, W.; Karger, B. L. *Anal. Chem.* **2001**, *73*, 1449−1454.
(18) Zhang, B. L.; Foret, F.; Karger, B. L. *Anal. Chem.* **2001**, *73*, 2675−2681.
(19) Wang, B.; Trimpin, S. *Anal. Chem.* **2014**, *86*, 1000−1006.
(20) Qiao, L.; Sartor, R.; Gasilova, N.; Lu, Y.; Tobolkina, E.; Liu, B.; Girault, H. *Anal. Chem.* **2012**, *84*, 7422−7430.
(21) Qiao, L.; Tobolkina, E.; Liu, B.; Girault, H. H. *Anal. Chem.* **2013**, *85*, 4745−4752.
(22) Qiao, L.; Tobolkina, E.; Lesch, A.; Bondarenko, A.; Zhong, X.; Liu, B.; Pick, H.; Vogel, H.; Girault, H. H. *Anal. Chem.* **2014**, *86*, 2033−2041.
(23) Tobolkina, E.; Qiao, L.; Xu, G.; Girault, H. H. *Rapid Commun. Mass Spectrom.* **2013**, *27*, 2310−2316.
(24) Qiao, L.; Sartor, R.; Gasilova, N.; Lu, Y.; Tobolkina, E.; Liu, B.; Girault, H. H. *Anal. Chem.* **2012**, *84*, 7422−7430.
(25) Golet, E. M.; Strehler, A.; Alder, A. C.; Giger, W. *Anal. Chem.* **2002**, *74*, 5455−5462.
(26) Hermo, M. P.; Nemutlu, E.; Kir, S.; Barron, D.; Barbosa, J. *Anal. Chim. Acta* **2008**, *613*, 98−107.
(27) Cancilla, M. T.; Leavell, M. D.; Chow, J.; Leary, J. A. *Proc. Natl. Acad. Sci. U. S. A.* **2000**, *97*, 12008−12013.
(28) Bertazzo, A.; Costa, C. V. L; Allegri, G.; Favretto, D.; Traldi, P. *J. Mass Spectrom.* **1999**, *34*, 922−929.
(29) Chang, T.-S. *Int. J. Mol. Sci.* **2009**, *10*, 2440−2475.
(30) Michaelis, L.; Menten, M. L. *Biochem Z.* **1913**, *49*, 333−369.
(31) Parvez, S.; Kang, M.; Chung, H.-S.; Bae, H. *Phytother. Res.* **2007**, *21*, 805−816.
(32) Kim, Y. J.; Uyama, H. *Cell. Mol. Life Sci.* **2005**, *62*, 1707−1723.
(33) Xie, L. P.; Chen, Q. X.; Huang, H. A.; Liu, X. D.; Chen, H. T.; Zhang, R. Q. *Int. J. Biochem. Cell Biol.* **2003**, *35*, 1658−1666.
(34) Lee, M. Y.; Park, C. B.; Dordick, J. S.; Clark, D. S. *Proc. Natl. Acad. Sci. U. S. A.* **2005**, *102*, 983−987.
(35) Ma, S. G.; Chowdhury, S. K. *Anal. Chem.* **2011**, *83*, 5028−5036.
(36) Bajrami, B.; Zhao, L. L.; Schenkman, J. B.; Rusling, J. F. *Anal. Chem.* **2009**, *81*, 9921−9929.
(37) Wang, X. D.; Li, J. L.; Lu, Y.; Chen, X.; Huang, M.; Chowbay, B.; Zhou, S. F. *J. Chromatogr. B: Anal. Technol. Biomed. Life Sci.* **2007**, *852*, 534−544.
(38) Choi, M. H.; Skipper, P. L.; Wishnok, J. S.; Tannenbaum, S. R. *Drug Metab. Dispos.* **2005**, *33*, 714−718.
(39) Tropsha, A. *Mol. Inf.* **2010**, *29*, 476−488.

DOI: 10.1021/acs.analchem.7b00536
Anal. Chem. 2017, 89, 5983−5990